AIAA Guidance, Navigation, and Control Conference
2 - 5 August 2010, Toronto, Ontario Canada

AIAA 2010-8044

An LMI-based Analysis for Adaptive Flight Control with Unmodeled Input Dynamics

Bong-Jun Yang,* Tansel Yucelen,†Jong-Yeob Shin,‡ Anthony J. Calise §

* Optimal Synthesis, Inc.

95 First Street, Los Altos,CA 94025

†,§ School of Aerospace Engineering, Georgia Institute of Technology

Atlanta, GA 30332

‡ Gulfstream Aerospace Corporation, Savannah, GA 31408

An LMI-based analysis is performed for adaptive control in the presence of unmodeled input dynamics. The formulation involves recasting the error dynamics composed of the tracking error and the weight estimation error into a linear parameter varying form. With the notion of $\mathcal{L}_2$ gain as a metric for robustness of adaptive control, we show that a broad class of unmodeled input dynamics can be analyzed under a previously developed LMI framework.

I. Introduction

Analyzing the robustness of an adaptive flight control system has been a very challenging problem. Standard adaptive control methods[1–6] employ time-varying parameters, which are updated in a nonlinear fashion, and traditional stability and robustness metrics developed for linear time-invariant (LTI) systems have been very difficult to apply. Moreover, the incorporation of time-varying adaptation laws fundamentally changes the characterization of stability from exponential stability to weaker assurance of either asymptotic stability of the tracking error,[3] which has been a fundamental obstacle in ensuring robustness of adaptive control.[7] The traditional validation procedure is based on linearized dynamics around a trim point and requires a closed-loop system to be exponentially stable,which ensures local exponential stability of original nonlinear systems due to Lyapunov's first theorem. In adaptive control, this can only be attained under a highly restrictive persistency of excitation condition. Consequently, it cannot not be claimed that adaptive control is robust to uncertainties that violate the parametrization assumed in the framework of adaptive control, such as unmatched uncertainties, unmodeled dynamics, external disturbances.[7]

Modification terms in adaptive laws, such as $\sigma-$modification,[8] $e-$modification,[1] and projection,[9] have been developed in an attempt to robustify the adaptive control process in the presence of uncertainties that violate the standard assumption in adaptive control. At the price of a weakened stability result, in which the tracking error is uniformly ultimate bounded(UUB)[10] rather than converge to zero, the incorporation of modification terms has been shown to tolerate a class of modeling errors.[3] The notion of UUBness has been particularly useful for neural network (NN)-based adaptive algorithms[10–12] because the inherent network approximation error necessitates the employment of modifications for proof of boundedness for closed-loop

*B.-J. Yang,Research Scientist, AIAA member, Email: jun.yang@optisyn.com
†T. Yucelen, Graduate Research Assistant, AIAA student member, Email:tansel@gatech.edu
‡J.Y. Shin, Research Scientist, AIAA member, Email:Jong.Yeob.Shin@gulfstream.com
§A. J. Calise, Professor, AIAA Fellow, Email: anthony.calise@ae.gatech.edu

Copyright © 2010 by the authors. Published by the American Institute of Aeronautics and Astronautics, Inc., with permission.

signals. In the case of a NN-based adaptive algorithm, this has been the price that one has to pay in order to eliminate the requirement of having a perfectly known regression vector. Nevertheless, a general analysis framework that provides a quantitative measure of the robustness of adaptive control systems to a broad class of uncertainties, such as an unstructured dynamic uncertainty, still remains as an open problem.

In Ref.s 13, 14 we have initiated an effort that addresses quantifying nominal system performance and stability margins of adaptive control using linear matrix inequality (LMI) tools. When an adaptive law with $\sigma-$modification is employed, the combined error dynamics, consisting of the tracking error and the weight estimate error can be decomposed into an exponentially stable system and a bounded perturbation. Then, it is shown that the exponentially stable system is cast as a linear-parameter varying (LPV) system, and therefore LMI analysis tools can be applied for the quantitative analysis of robustness. Ref.14 shows that using the small-gain theorem in an $\mathcal{L}_2$ setting permits the size of tolerable uncertain dynamic mappings to be specified by their $\mathcal{L}_2$ gain. Subsequently, this $\mathcal{L}_2$ gain is utilized to derive guaranteed gain and time-delay margins in the input channel. Ref. 15 applies $\mathcal{L}_2$ gain analysis to quantify the size of a tolerable state-dependent unmatched uncertainty in adaptive control.

In this paper, we show that the $\mathcal{L}_2$ gain analysis framework developed in Ref.14 can also be applied to quantify tolerable unmodeled input dynamics that can either be matched or unmatched. Following Ref.s 13–15, the combined error dynamics, composed of the tracking error and the weight estimate error, are cast as an exponentially stable system under bounded perturbation by employing $\sigma-$modification as an essential ingredient.[13,14] The exponentially perturbed system is then viewed as a linear-parameter varying (LPV) system, and LMI analysis tools are applied to analyze robustness of adaptive control to unmodeled input dynamics.

The paper is organized as follows. In Section II the $\mathcal{L}_2$ gain is formulated as a measure of robustness to unmodeled input dynamics. In Section III, LMI analysis is presented. In Section IV, LMI analysis is applied to Rohrs' example and the Generic Transportation Model (GTM) example and derives the disk margin ($\mathcal{L}_2$ gain). The guaranteed disk margin is verified in simulations. Conclusions are given in Section V.

II. Problem Formulation

A. Preliminary

Consider a single-input single-output (SISO) system described by:

$$\begin{aligned} \dot{\boldsymbol{x}} =& A\boldsymbol{x} + \boldsymbol{b}(u + \boldsymbol{W}^\top \boldsymbol{\phi}(\boldsymbol{x})), \\ y =& \boldsymbol{c}^\top \boldsymbol{x}, \end{aligned} \tag{1}$$

where $\boldsymbol{x} \in \mathbb{R}^n$ is the system state vector, $u \in \mathbb{R}$ is the input, $y \in \mathbb{R}$ is the output, $\boldsymbol{W} \in \mathbb{R}^N$ is a uncertain parameter vector, $\boldsymbol{\phi}(\boldsymbol{x}) \in \mathbb{R}^N$ is a known set of smooth basis functions, and the system matrices $A, \boldsymbol{b}, \boldsymbol{c}^\top$ are known. A nominal linear controller:

$$u_{nom} = -\boldsymbol{K}_x^\top \boldsymbol{x} + K_r r, \tag{2}$$

is assumed to be designed such that the resulting closed-loop system with the known part of the system in (1) satisfies design specifications. Hence we can define a reference model for the desired behavior using

$$\begin{aligned} \dot{\boldsymbol{x}}_m =& A_m \boldsymbol{x}_m + \boldsymbol{b}_m r \\ y_m =& \boldsymbol{c}^\top \boldsymbol{x}_m, \end{aligned} \tag{3}$$

where $A_m = A - \boldsymbol{b}\boldsymbol{K}_x^\top$ is Hurwitz, $\boldsymbol{b}_m = \boldsymbol{b}K_r$, and r is a bounded reference command.

Let

$$u = u_{nom} - u_{ad}, \tag{4}$$

where u_{ad} is an adaptive signal introduced to approximately cancel the uncertainty $\boldsymbol{W}^\top \boldsymbol{\phi}(\boldsymbol{x})$:

$$u_{ad} = \widehat{\boldsymbol{W}}^\top \boldsymbol{\phi}(\boldsymbol{x}), \tag{5}$$

whose estimate $\widehat{\boldsymbol{W}}$ for the ideal weight $\boldsymbol{W}$ in (1) is updated using:

$$\dot{\widehat{\boldsymbol{W}}} = -\gamma \boldsymbol{\phi}(\boldsymbol{x}) \boldsymbol{e}^\top P \boldsymbol{b} - \sigma \widehat{\boldsymbol{W}}, \tag{6}$$

where $\gamma > 0 \in \mathbb{R}$ is the adaptation gain, σ is the $\sigma-$modification gain, and $P > 0$ is obtained by solving the following Lyapunov function with a selected $Q > 0$:

$$A_m^\top P + P A_m + Q = 0, \tag{7}$$

and $\boldsymbol{e}$ is the tracking error given by:

$$\boldsymbol{e} = \boldsymbol{x}_m - \boldsymbol{x}. \tag{8}$$

The tracking error dynamics are described by:

$$\dot{\boldsymbol{e}} = A_m \boldsymbol{e} + \boldsymbol{b} \widetilde{\boldsymbol{W}}^\top \boldsymbol{\phi}(\boldsymbol{x}), \tag{9}$$

where $\widetilde{\boldsymbol{W}} = \widehat{\boldsymbol{W}} - \boldsymbol{W}$ is the weight estimation error. From (6), the weight estimation error dynamics can be written as

$$\dot{\widetilde{\boldsymbol{W}}} = -\gamma \boldsymbol{\phi}(\boldsymbol{x}) \boldsymbol{e}^\top P \boldsymbol{b} - \sigma \widetilde{\boldsymbol{W}} - \sigma \boldsymbol{W}. \tag{10}$$

Let

$$\boldsymbol{\zeta} = [\boldsymbol{e}^\top, \widetilde{\boldsymbol{W}}^\top]^\top. \tag{11}$$

Then the error dynamics composed of the tracking error and the weight estimation error are described by:

$$\begin{aligned} \dot{\boldsymbol{\zeta}} &= \underbrace{\begin{bmatrix} A_m & \boldsymbol{b}\boldsymbol{\phi}(\boldsymbol{x})^\top \\ -\gamma \phi(\boldsymbol{x}) \boldsymbol{b}^\top P & -\sigma I_N \end{bmatrix}}_{\bar{A}(\boldsymbol{x})} \boldsymbol{\zeta} + \underbrace{\begin{bmatrix} 0 \\ -\sigma I_N \end{bmatrix}}_{\bar{B}} \boldsymbol{W} \\ \boldsymbol{e} &= \underbrace{\begin{bmatrix} I_n & \boldsymbol{0}_{n \times N} \end{bmatrix}}_{\bar{C}_e} \boldsymbol{\zeta}. \end{aligned} \tag{12}$$

In the literature, a stability analysis for the system in (12) is typically carried out by considering the following Lyapunov candidate function:

$$V(\boldsymbol{\zeta}) = \boldsymbol{e}^\top P \boldsymbol{e} + \frac{1}{\gamma} \widetilde{\boldsymbol{W}}^\top \widetilde{\boldsymbol{W}} = \boldsymbol{\zeta}^\top X_0 \boldsymbol{\zeta}, \tag{13}$$

where

$$X_0 = \begin{bmatrix} P & 0 \\ 0 & \gamma^{-1} I_N \end{bmatrix}. \tag{14}$$

The time derivative of V along with (19) reduces to:

$$\begin{aligned} \dot{V} &= -\boldsymbol{e}^\top Q \boldsymbol{e} - 2 \frac{\sigma}{\gamma} \widetilde{\boldsymbol{W}}^\top \widehat{\boldsymbol{W}} \\ &= -\boldsymbol{e}^\top Q \boldsymbol{e} - \frac{\sigma}{\gamma} [\left\| \widetilde{\boldsymbol{W}} \right\|^2 + \left\| \widehat{\boldsymbol{W}} \right\|^2 - \|\boldsymbol{W}\|^2] \\ &\leq -\lambda_{\min}(Q) \|\boldsymbol{e}\|^2 - \frac{\sigma}{\gamma} \left\| \widetilde{\boldsymbol{W}} \right\|^2 + \frac{\sigma}{\gamma} \|\boldsymbol{W}\|^2 \\ &\leq -\mu \|\boldsymbol{\zeta}\|^2 + \frac{\sigma}{\gamma} \|\boldsymbol{W}\|^2, \end{aligned} \tag{15}$$

where $\mu = \min\{\lambda_{\min}(Q), \frac{\sigma}{\gamma}\}$. Whenever $\|\boldsymbol{\zeta}\| \geq \sqrt{\frac{\sigma}{\gamma \mu}} \|\boldsymbol{W}\|$, $\dot{V} \leq 0$. Hence, $\boldsymbol{\zeta}$ is UUB.[16] Note that due to $\sigma-$modification, only the UUBness of the closed-loop signals is guaranteed. However, the adaptive system remains bounded when subject to additional bounded external disturbances.[8]

Remark 1. In this paper we formulate the problem in a SISO setting for seamless extension from the result in Ref.14 as well as for the ease of presentation. While the gain and phase margin are developed in a SISO LTI setting, the notion of $\mathcal{L}_2$ gain is well defined regardless of the number of inputs and outputs. This implies that the $\mathcal{L}_2$ gain analysis presented in this paper can also be applied to multi-input multi-output problems.

B. Uncertain Input Dynamics

The viewpoint taken in Ref.s 13, 14 is that the system in (12) can be viewed as an exponentially stable system (due to exponentially stable $\bar{A}(\boldsymbol{x})$)) perturbed by the external disturbance $\boldsymbol{W}$. In Ref.14, in order to obtain allowable gain variation and time delay in the input channel, a system for which the controller in (5) is designed using the model in (1) is assumed to have an uncertain dynamic mapping in the feedback interconnection form shown in Figure 1. It is straightforward to show that the following system for an

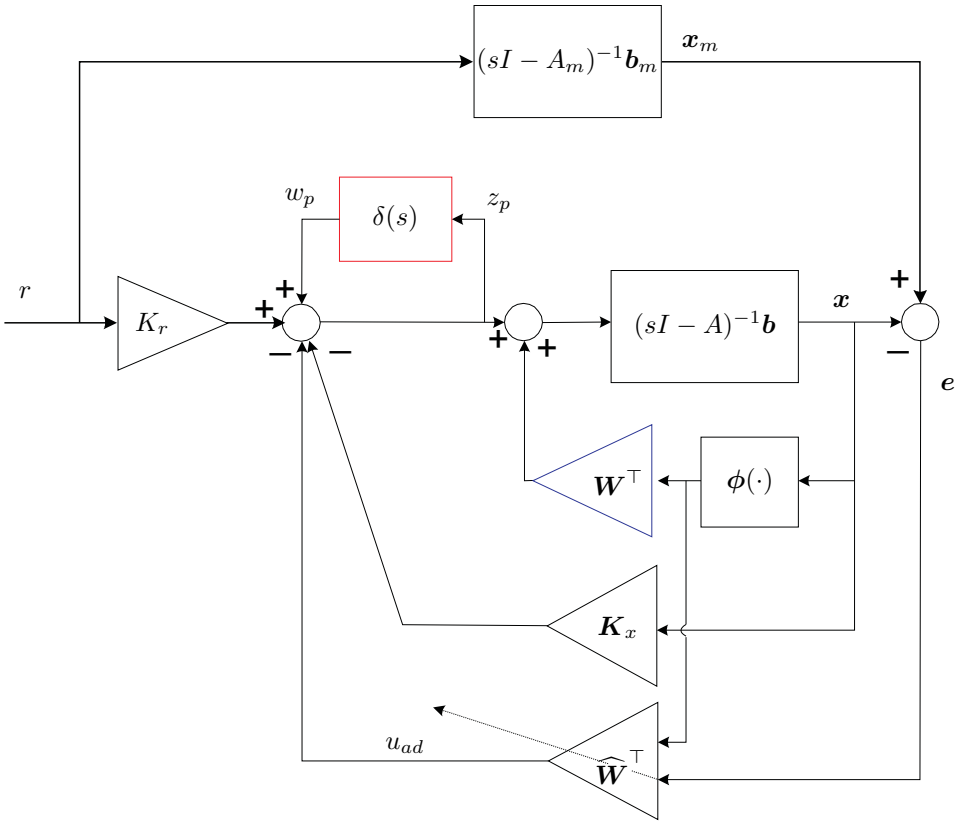

Figure 1. Adaptive control with uncertainty in the input channel

uncertain system:

$$\dot{\boldsymbol{x}} = A\boldsymbol{x} + \boldsymbol{b}(u + \delta(s)u + \boldsymbol{W}^\top \boldsymbol{\phi}(\boldsymbol{x})), \tag{16}$$

where the Laplace variable s is employed to denote that $\delta(s)$ is a SISO transfer function, can also lead to the same result in Ref.14. The procedure for obtaining guaranteed gain and time-delay margin[17] involves first specifying the size of the uncertain mapping $\delta(s)$ in terms of $\mathcal{L}_2$ gain, which is referred as the disk margin.[18,19] In other words, in Ref. 14, the $\mathcal{L}_2$ gain analysis is carried out for the case of SISO unmodeled input dynamics that enter the system dynamics at the same location as the control input.

The class of systems considered in Ref.15 is defined by:

$$\begin{aligned}\dot{\boldsymbol{x}} =& A\boldsymbol{x} + \boldsymbol{b}(u + \boldsymbol{W}^\top \boldsymbol{\phi}(\boldsymbol{x})) + B_u \boldsymbol{\Delta}_u(\boldsymbol{z}),\\ \boldsymbol{z} =& C_u \boldsymbol{x}\\ y =& \boldsymbol{c}^\top \boldsymbol{x},\end{aligned} \tag{17}$$

where B_u and C_u are known. $\mathcal{L}_2$ gain analysis is performed to quantify the size of the tolerable state-dependent unmatched uncertainty $\boldsymbol{\Delta}_u(\boldsymbol{z})$.

In this paper, we explore the validity of the $\mathcal{L}_2$ gain analysis as a way to quantify an uncertain input mapping that may enter the system in locations different from the nominal control channel. This paper is concerned with the system described by:

$$\begin{aligned}\dot{\boldsymbol{x}} =& A\boldsymbol{x} + \boldsymbol{b}(u + \boldsymbol{W}^\top \boldsymbol{\phi}(\boldsymbol{x})) + B_u \Delta(t,u),\\ y =& \boldsymbol{c}^\top \boldsymbol{x},\end{aligned} \tag{18}$$

where $B_u \in \mathbb{R}^{n\times p}$ is known constant matrix, and $\Delta(t,u)$ is a $p\times 1$ dynamic mapping. Note that the class in (18) includes unmatched input unmodeled dynamics. In other words, the problem solved in this paper is:

> What is the size of unmodeled input dynamics in (18) that can be tolerated by the control law in (4) when the channel B_u is known?

The size is specified by the $\mathcal{L}_2$ gain following the approaches taken in Ref.s 14 and 15.

III. LMI Analysis

Following the steps in Section II-A, applying the controller in (4) to the system in (18) leads to the following error dynamics:

$$\begin{aligned}\dot{\boldsymbol{\zeta}} =& \underbrace{\begin{bmatrix} A_m & \boldsymbol{b}\boldsymbol{\phi}(\boldsymbol{x})^\top \\ -\gamma\phi(\boldsymbol{x})\boldsymbol{b}^\top P & -\sigma I_N \end{bmatrix}}_{\bar{A}(\boldsymbol{x})} \boldsymbol{\zeta} + \underbrace{\begin{bmatrix} -B_u \\ 0 \end{bmatrix}}_{\bar{B}_p} \boldsymbol{w}_p + \underbrace{\begin{bmatrix} 0 \\ -\sigma I_N \end{bmatrix}}_{\bar{B}_w} \boldsymbol{W}\\ \boldsymbol{w}_p =& \Delta(t,u),\\ \boldsymbol{e} =& \underbrace{\begin{bmatrix} I_n & \boldsymbol{0}_{n\times N} \end{bmatrix}}_{\bar{C}_e} \boldsymbol{\zeta}.\end{aligned} \tag{19}$$

The control signal u is given by:

$$\begin{aligned}u &= K_r r - \boldsymbol{K}_x \boldsymbol{x} - \widehat{\boldsymbol{W}}^\top \boldsymbol{\phi}(\boldsymbol{x})\\ &= K_r r - \boldsymbol{K}_x(\boldsymbol{x}_m - \boldsymbol{e}) - \widetilde{\boldsymbol{W}}^\top \boldsymbol{\phi}(\boldsymbol{x}) - \boldsymbol{W}^\top \boldsymbol{\phi}(\boldsymbol{x}).\end{aligned} \tag{20}$$

Let $f(\boldsymbol{x}) = \boldsymbol{W}^\top \boldsymbol{\phi}(\boldsymbol{x})$. Then, by the mean value theorem, we have:

$$\begin{aligned}f(\boldsymbol{x}) &= f(\boldsymbol{x}_m) - \frac{\partial f}{\partial \boldsymbol{x}}\Big|_{\bar{\boldsymbol{x}}} \boldsymbol{e}\\ &= \boldsymbol{W}^\top \boldsymbol{\phi}(\boldsymbol{x}_m) - \boldsymbol{W}^\top \boldsymbol{\phi}_x(\bar{\boldsymbol{x}})\boldsymbol{e}.\end{aligned} \tag{21}$$

where $\bar{\boldsymbol{x}} = \boldsymbol{x}_m + \theta \boldsymbol{e},\ \theta \in [0,1]$. The resulting error dynamics can be described by:

$$\begin{aligned} \dot{\boldsymbol{\zeta}} &= \bar{A}(x)\boldsymbol{\zeta} + \bar{B}_p \boldsymbol{w}_p + \bar{B}_w \boldsymbol{w}_0 \\ z_1 &= \underbrace{\left[\begin{array}{cc} \boldsymbol{K}_x^\top + \boldsymbol{W}^\top \boldsymbol{\phi}_x(\bar{\boldsymbol{x}}) & -\boldsymbol{\phi}(\boldsymbol{x})^\top \end{array}\right]}_{\bar{C}_p(\bar{\boldsymbol{x}},\boldsymbol{x})} \boldsymbol{\zeta}, \\ z_p &= z_1 + z_0, \\ \boldsymbol{w}_p &= \Delta(t, z_p), \end{aligned} \tag{22}$$

where $z_p := u$, $\boldsymbol{w}_0 = \boldsymbol{W}$, and $z_0 = K_r r - \boldsymbol{K}_x^\top \boldsymbol{x}_m - \boldsymbol{W}^\top \boldsymbol{\phi}(\boldsymbol{x}_m)$. We note that $w_0, z_0 \in \mathcal{L}_\infty \cap \mathcal{L}_{2_e}$ because r and $\boldsymbol{x}_m$ are bounded for $\forall t \geq 0$. By introducing the following system

$$\Sigma \sim \left[\begin{array}{ccc} \bar{A}(\boldsymbol{x}) & \bar{B}_p & \bar{B}_w \\ \bar{C}_p(\bar{\boldsymbol{x}}, \boldsymbol{x}) & 0 & 0 \end{array}\right],$$

whose inputs and outputs are $(\boldsymbol{w}_o, \boldsymbol{w}_p)$ and z_1, respectively, the overall closed loop system in (22) can be described as the feedback interconnection depicted in Figure 2. We notice that the error dynamics in (22)

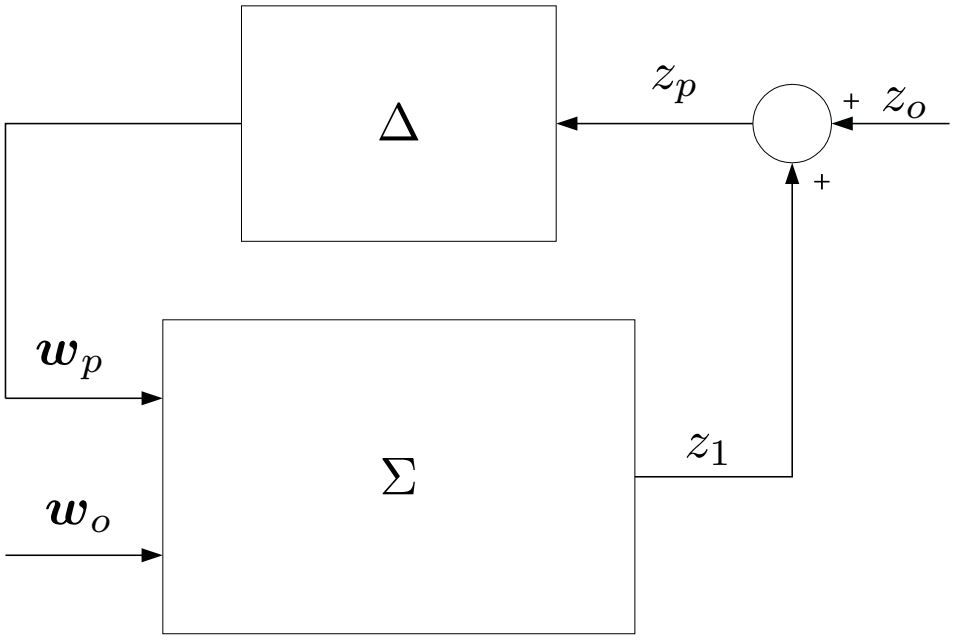

Figure 2. Interconnection with the pull-out of the uncertainty

have exactly the same form as considered in Ref.14, and therefore the same analysis procedure can be applied.

A. Affine Parametrization

Let Ω_x be a compact set of interest such that $\boldsymbol{x}(t) \in \Omega_x$ for all $t \geq 0$. Define the following parameter vector:

$$\boldsymbol{\rho}^a = \left[\begin{array}{c} \boldsymbol{\phi}(\boldsymbol{x}) \\ \boldsymbol{W}^\top \boldsymbol{\phi}_x(\bar{\boldsymbol{x}}) \end{array}\right] \in \mathbb{R}^{N+n} \tag{23}$$

and a set to which the parameter belongs:

$$\mathcal{P}^a := \{\boldsymbol{\rho}^a = (\rho_1^a, \ldots, \rho_{N+n}^a)\ :\ \rho_i^a \in [\underline{\rho}_j^a, \overline{\rho}_j^a]\}, \tag{24}$$

whose corners belong to the following set:

$$\mathcal{P}_0^a := \left\{ \boldsymbol{\rho}^a = (\rho_1^a, \ldots, \rho_{N+n}^a) \ : \ \rho_i^a \in \{\underline{\rho}_j^a, \overline{\rho}_j^a\} \right\}. \tag{25}$$

In other words, the parameter set $\mathcal{P}^a$ is the convex hull of the set of corners $\mathcal{P}_0^a$, i.e, $\mathcal{P}^a = co(P_0^a)$. The corners of the first N parameters are found by $\underline{\rho}_j^a = \min(\phi_j(\boldsymbol{x}))$, $\overline{\rho}_j^a = \max(\phi_j(\boldsymbol{x})), 1 \leq j \leq N$, on the known compact set Ω_x. The other parameter $\boldsymbol{W}^\top \boldsymbol{\phi}_x(\bar{\boldsymbol{x}}(t)))$ is unknown because it involves the unknown parameter $\boldsymbol{W}$ and the unknown variable $\bar{\boldsymbol{x}}$. It is assumed that the uncertainty satisfies a linear growth assumption.

Assumption 1. $\left\| \frac{\partial}{\partial \boldsymbol{x}} \boldsymbol{W}^\top \boldsymbol{\phi}(\boldsymbol{x}) \right\| \leq w^*$ for $\forall \boldsymbol{x} \in \Omega_x$.

Since $\bar{\boldsymbol{x}}(t) = \boldsymbol{x}_m(t) + \theta \boldsymbol{e}(t)$ with $\theta \in [0,1]$ and $\bar{\boldsymbol{x}}(t) \in \Omega_x$ as long as $\boldsymbol{x}(t) \in \Omega_x$, Assumption 1 ensures that $\left\| \boldsymbol{W}^\top \boldsymbol{\phi}_x(\bar{\boldsymbol{x}}(t)) \right\| \leq w^*$. Then $|\rho_j^a| \leq \|\rho^a(N+1:N+n)\|_\infty \leq \|\rho^a(N+1:N+n)\| \leq w^*$. This leads to $\underline{\rho}_j^a = -w^*, \overline{\rho}_j^a = w^*$ for $\forall N+1 \leq j \leq N+n$. With the parameter vector $\boldsymbol{\rho}^a$, we have

$$\begin{aligned} \bar{A}(\boldsymbol{x}) &= \bar{A}(\boldsymbol{\rho}^a) = A_0 + \sum_{j=1}^{N} \rho_j^a A_j, \\ \bar{C}_p(\boldsymbol{\rho}^a) &= C_0 + \sum_{j=1}^{N+n} \rho_j^a C_j, \end{aligned} \tag{26}$$

where $A_0 = \begin{bmatrix} A_m & \boldsymbol{0}_{n\times N} \\ \boldsymbol{0}_{N\times n} & -\sigma I_N \end{bmatrix}$, $A_j \in \mathbb{R}^{(n+N)\times(n+N)}$ is a matrix such that $A_j(1:n,k) = \boldsymbol{b}$, $A_j(k,1:n) = -\gamma \boldsymbol{b}^\top P$ if $k = j$, and $A_j(k,l) = 0$ otherwise ($k \neq j$ nor $l \neq j$), $C_0 = \begin{bmatrix} -\boldsymbol{K}_x & \boldsymbol{0}_{1\times N} \end{bmatrix}$, $C_j \in \mathbb{R}^{1\times(N+n)}$ such that $C_j(n+k) = -1$ if $k = j$, and $C_j(k) = 0$ otherwise for $1 \leq j \leq N$, and $C_j(k) = -1$ if $k = N+j$, $C_j(k) = 0$ otherwise for $N+1 \leq j \leq N+n$. The notation $1:n$ is used to represent indices from 1 to n.

B. $\mathcal{L}_2$ gain analysis

The size of tolerable input unmodeled dynamics is quantified by the following Lemma.

Lemma 1. Suppose that we solve the following LMI problem:

$$\begin{aligned} &\textit{minimize } \gamma_s > 0 \text{ subject to} \\ &\quad X = X^\top > 0 \text{ and} \\ &\begin{bmatrix} \bar{A}(\boldsymbol{\rho}^a)^\top X + X\bar{A}(\boldsymbol{\rho}^a) + \bar{C}_p^\top \bar{C}_p & X\bar{B}_p \\ \bar{B}_p^\top X & -\gamma_s^2 I \end{bmatrix} < 0, \ \forall \boldsymbol{\rho}^a \in \mathcal{P}_0^a. \end{aligned} \tag{27}$$

Then, the closed loop system in (22), depicted in Figure 2, remains stable for all the uncertain mapping $\boldsymbol{\Delta}$ whose $\mathcal{L}_2$ gain is less than $1/\gamma_s$.

The proof of Lemma 1 follows directly from the small-gain theorem[20] and the fact that $A(\boldsymbol{\rho}^a)$ is affinely parameterized with respect to $\boldsymbol{\rho}^a$. The lemma establishes that the adaptive closed loop system remains stable in the presence of *any* uncertain, dynamic or static mapping $\boldsymbol{\Delta}(t,u)$ whose $\mathcal{L}_2$ gain is less than $1/\gamma_s$.

IV. Simulations

A. Rohrs' Example

Consider the following system:

$$y(s) = \frac{2}{s+1} \underbrace{\frac{229\alpha}{s^2+30s+229}}_{\eta(s)} u(s), \tag{28}$$

where $\eta(s)$ represents unmodeled input dynamics. The parameter α is introduced as a scale factor. The system with $\alpha = 1$ was considered in Ref.7 in order to illustrate the loss of robustness of Model Reference Adaptive Control (MRAC) to unmodeled dynamics, which has led to later development of modification terms.[1,8,9]

The plant model considered in the design of a linear controller is described by:

$$\dot{x} = -x + 2u. \tag{29}$$

The linear controller is given by:

$$u_{\text{nom}} = -x + \frac{3}{2}r. \tag{30}$$

The nominal closed-loop system constitutes the following reference model

$$\dot{x}_m = -3x_m + 3r. \tag{31}$$

As in Ref.7, the reference command r is set as

$$r = 0.3 + 1.85\sin(16.1t). \tag{32}$$

Since the true dynamics in (28) are unknown, an adaptive controller is designed under the assumption that the true plant is represented by:

$$\dot{x} = -x + 2(u + Wx), \tag{33}$$

where $x(= \phi(x))$ is the known regression vector and $W = 0$ is unknown. The adaptive control signal is given by:

$$u_{ad} = \widehat{W}x, \tag{34}$$

where $\widehat{W}$ is the estimate for the unknown constant W and is updated by

$$\dot{\widehat{W}} = -\frac{2}{3}\gamma x e - \sigma\widehat{W}, \tag{35}$$

where $e = x_m - x$. Compared to the weight update law in (6), the update law implies that $P = 1/3$, which is obtained from (7) with $Q = 2$. Figure 3 shows the time responses of the tracking error e and the Lyapunov candidate function V in (13) in the absence of unmodeled dynamics $\eta(s)$ with adaptive parameters $(\gamma, \sigma) = (10, 1)$. Both the tracking error and the weight estimation error converges to zero.

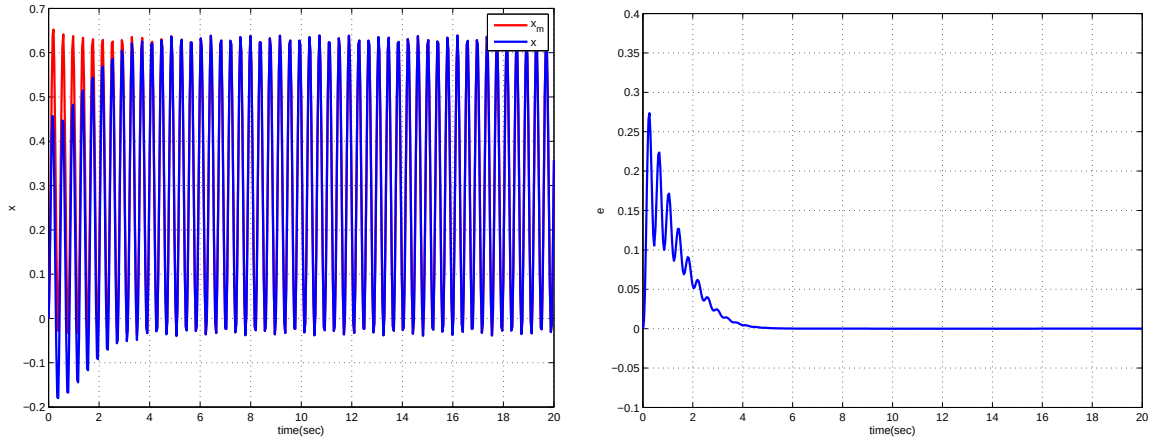

(a) Time response of x (b) Tracking error response

Figure 3. Adaptive control responses with $\gamma = 10$ and $\sigma = 1.0$

With the control law in (4), if the system in (33) were the true dynamics, the resulting combined error dynamics would be described by

$$\dot{\boldsymbol{\zeta}} = \begin{bmatrix} -3 & 2x \\ -\frac{2}{3}\gamma x & -\sigma \end{bmatrix} \boldsymbol{\zeta} + \begin{bmatrix} 0 \\ -\sigma \end{bmatrix} W, \tag{36}$$

where $\boldsymbol{\zeta} = [e, \widetilde{W}]^\top$. The error dynamics in (36) represents a typical form considered in the standard stability analysis. However, the true dynamics are given in (28) and are different from the system (33) that is considered in the design of adaptive control. Compared to the system (33), the true dynamics are given by:

$$\dot{x} = -x + 2(u + Wx) + 2\delta(s)u, \tag{37}$$

where $\delta(s) = \eta(s) - 1 = -\frac{s^2+30s+229(1-\alpha)}{s^2+30s+229}$ represents the unmodeled input dynamics. The magnitude of frequency responses of $\delta(s)$ with varying α is illustrated in Figure 4(a). Figure 4(b) shows that the H_∞ norm ($= \max_{\omega\in\mathbb{R}} |\delta(j\omega)|$) is a monotonic function of the scale factor α, which enables us to investigate the validity of guaranteed $\mathcal{L}_2$ gain by adjusting the scale factor. With the true system in (37), the combined

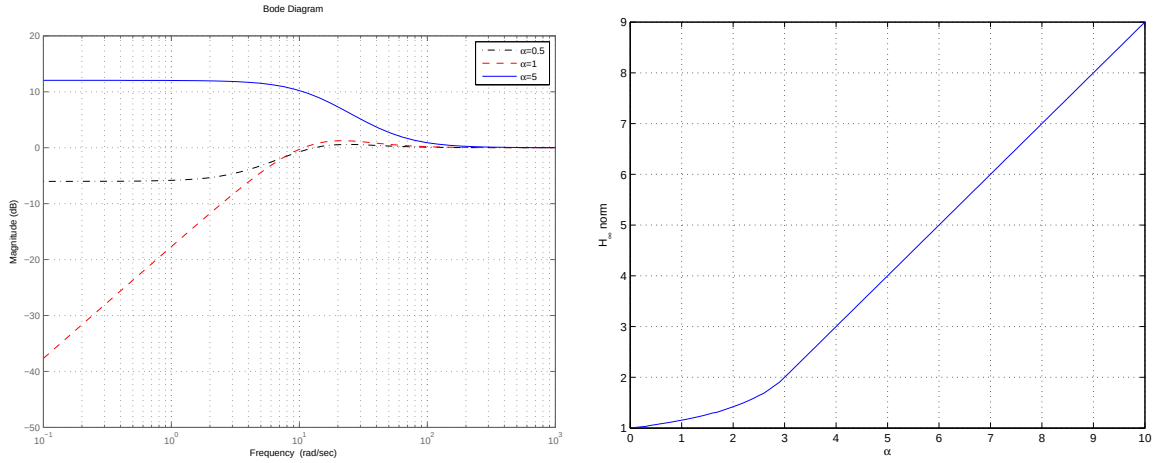

(a) Frequency magnitude responses

(b) H_∞ norm vs the scaling factor α

Figure 4. H_∞ norm variation of $\delta(s)$ with varying scaling factor

error $\boldsymbol{\zeta}$ evolves according to:

$$\begin{aligned} \dot{\boldsymbol{\zeta}} &= \begin{bmatrix} -3 & 2x \\ -\frac{2}{3}\gamma x & -\sigma \end{bmatrix} \boldsymbol{\zeta} + \begin{bmatrix} -2 \\ 0 \end{bmatrix} w_p + \begin{bmatrix} 0 \\ -\sigma \end{bmatrix} W, \\ w_p &= \delta(s)(z_1 + z_0), \\ z_1 &= \begin{bmatrix} 1+W & x \end{bmatrix} \boldsymbol{\zeta}, \\ z_0 &= \frac{3}{2} r - x_m - W x_m. \end{aligned} \tag{38}$$

For affine parametrization, considering that the adaptive control signal with $\gamma = 10$ and $\sigma = 1.0$ ensures that $x \in [-0.2, 0.7]$ with the reference command r in (32), the compact set Ω_x is set as $[-1, 1]$. Also $W(=0)$ is assumed to belong to the interval $[-0.1, 0.1]$. This leads to the set of corners in (25) as

$$\mathcal{P}_0^a := \{\boldsymbol{\rho}^a = (x, W) \ : \ x \in \{-1, 1\}, \ W \in \{-0.1, 0.1\}\}. \tag{39}$$

The disk margins ($\mathcal{L}_2$ gain) obtained by applying Lemma 1 with varying adaptation gains and $\sigma-$modification gains are given in Table 1. It is interesting that almost the same disk size is obtained for the same ratio

	$\gamma = 0.1$	$\gamma = 1$	$\gamma = 10$	$\gamma = 100$
$\sigma = 0.01$	1.0057	0.2994	0.0944	0.0299
$\sigma = 0.1$	1.3614	1.0062	0.2999	0.0946
$\sigma = 1.0$	1.3627	1.3620	1.0070	0.2997
$\sigma = 10$	1.3616	1.3628	1.3626	1.0061

Table 1. Tolerable disk size $1/\gamma_s$

between γ and σ. In the Rohrs' example with $\alpha = 1$, the $\mathcal{L}_2$ gain for $\delta(s)$ is 1.1554, and therefore any (γ, σ) whose tolerable disk size is larger than 1.1554 will not incur instability. In Table 1, any (γ, σ) belonging to lower triangular sections of the table are guaranteed not to destroy the stability of the adaptive closed loop system. For example, Figure 5 demonstrates that the time response of the Lyapunov candidate function in (13) is indeed bounded for the cases of $(\gamma, \sigma) = (1, 1), (1, 10)$.

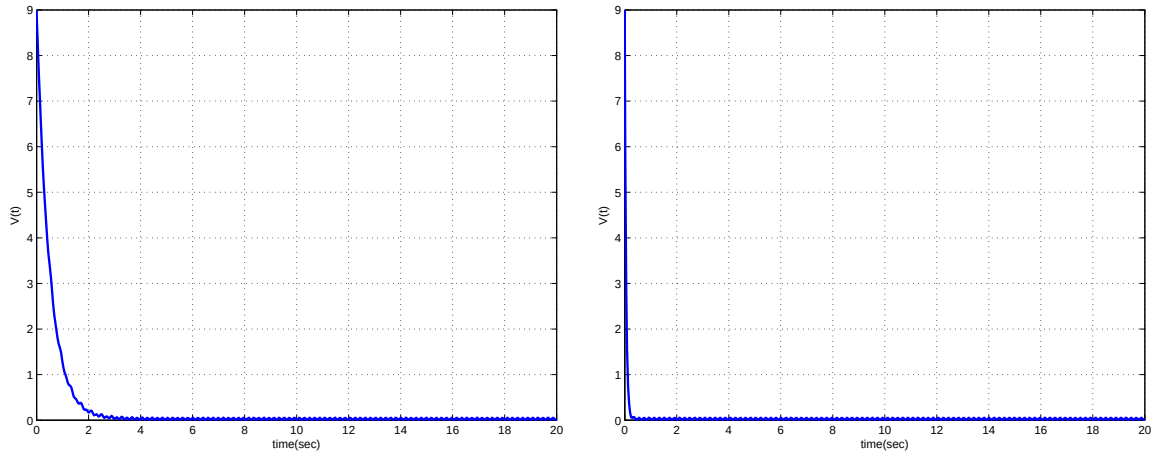

(a) Time response of V with $\gamma = 1$ and $\sigma = 1$

(b) Time response of V with $\gamma = 1$ and $\sigma = 10$

Figure 5. Time responses of the Lyapunov candidate function in (13)

Since the results given in Table 1 represents only a sufficient condition for stability of the adaptive control system, the results cannot be used to predict if the adaptive control system go unstable when the $\mathcal{L}_2$ gain of $\delta(s)$ is larger than $1/\gamma_s$. Figure 6(a) illustrates this point by showing that V remains bounded when the $\|\delta(s)\|_\infty = 1.1554 > 1/\gamma_s = 1.0007$ with $(\gamma, \sigma) = (10, 1)$. The conservatism associated with the tolerable size is investigated by finding the value α beyond which the adaptive system goes unstable. With $(\gamma, \sigma) = (10, 1)$, the α value greater than 2.4 renders the closed-loop system unstable. Figure 6(b) shows the time response of V when $\alpha = 2.4$ ($\|\delta(s)\|_\infty = 1.5889$). The scale factor α values and the corresponding H_∞ norms beyond which the closed-loop system goes unstable in stimulation are tabulated in Table 2. Those values are obtained by a trial and error process that involves adjusting α in simulations. Note that the guaranteed disk margin

	$\gamma = 0.1$	$\gamma = 1$	$\gamma = 10$	$\gamma = 100$
$\sigma = 0.01$	2.8(1.8319)	1.9(1.3856)	0.9(1.1367)	0.8(1.1189)
$\sigma = 0.1$	3.4(2.4000)	2.4(1.5889)	1.4(1.2419)	0.9(1.1367)
$\sigma = 1.0$	5.6(4.6000)	3.9(2.9000)	2.4(1.5889)	1.3(1.2183)
$\sigma = 10$	10.5(9.5000)	7.3(6.3000)	4.3(3.3000)	2.3(1.5412)

Table 2. The scaling factor α and the corresponding disk size obtained by trial and error in simulations

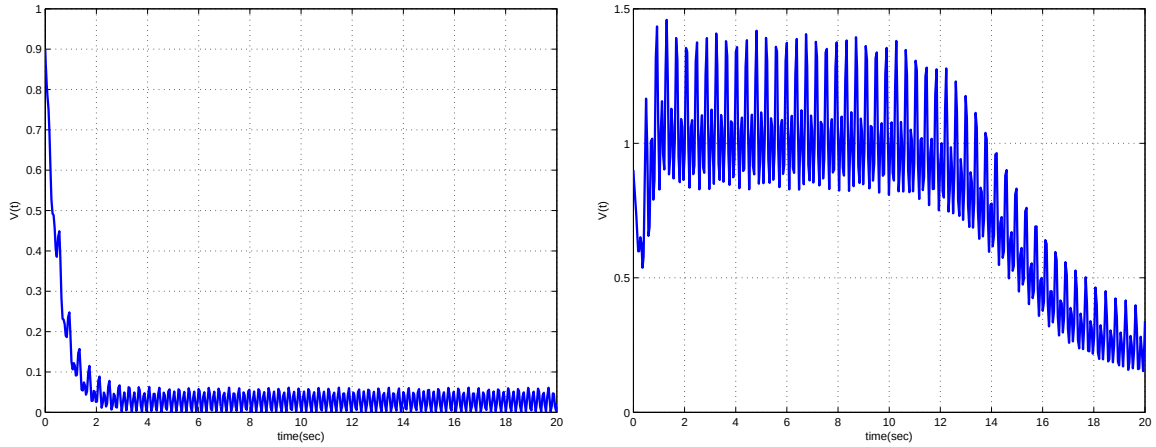

(a) when $\alpha = 1$ (b) when $\alpha = 2.4$

Figure 6. Time responses of V with $(\gamma, \sigma) = (10, 1)$

in Table 1 becomes less conservative as the ratio between the adaptation gain and the $\sigma-$modification tends towards 10. As the ratio of (γ, σ) move away from 10, the theoretical results tends to be more conservative.

B. Roll rate tracking using GTM

Consider GTM lateral dynamics described by:

$$\begin{aligned} \dot{\boldsymbol{x}} &= A\boldsymbol{x} + \alpha \boldsymbol{b} u + \boldsymbol{b}_m p_{cmd}, \\ y &= \boldsymbol{c}^\top \boldsymbol{x} \end{aligned} \tag{40}$$

where the state vector $\boldsymbol{x} = [p_i, v, p, r]$ is composed of an integrator of the roll rate error, the $Y-$axis velocity, the roll rate, and the yaw rate, respectively. The output y represents the roll rate, the control signal $u = \delta_a$ represents the aileron deflection, and p_{cmd} represents the roll rate reference command. The parameter α is introduced as a scale factor in order to adjust the size ($\mathcal{L}_2$ gain) of the unmodeled dynamics in the simulation. The case $\alpha = 1$ corresponds to the dynamics obtained by linearizing the GTM model at the angle of attack 2^o trim point. The system matrices are given by:

$$A = \begin{bmatrix} 0 & 0 & -1 & 0 \\ 0 & -0.8532 & 6.5778 & -186.3175 \\ 0 & -0.8720 & -8.7068 & 1.9306 \\ 0 & 0.3365 & -0.2895 & -2.0953 \end{bmatrix}, \boldsymbol{b} = \begin{bmatrix} 0 \\ -0.0665 \\ -1.7828 \\ -0.0462 \end{bmatrix}, \boldsymbol{c} = \begin{bmatrix} 0 \\ 0 \\ 1 \\ 0 \end{bmatrix}, \boldsymbol{b_m} = \begin{bmatrix} 1 \\ 0 \\ 0 \\ 0 \end{bmatrix}. \tag{41}$$

The nominal controller in (2) is designed as a linear quadratic regulator (LQR) whose feedback and feedforward gains are:

$$\boldsymbol{K}_x^\top = \begin{bmatrix} 100.0000 & 0.3868 & -6.5963 & -5.3349 \end{bmatrix}, \; K_r = 0. \tag{42}$$

The reference model in (3) is realized as a nominal closed loop system in which the known part of the linear system in (40) is regulated by the LQR controller. It is given by:

$$\dot{\boldsymbol{x}}_m = A_m \boldsymbol{x}_m + \boldsymbol{b}_m p_{cmd}, \tag{43}$$

where $A_m = A - \alpha \boldsymbol{b} K_x^\top$. Notice that the reference model also changes as the scale factor α varies. When $\alpha = 1$, the closed-loop system has gain margin (GM) of infinity, the phase margin (PM) of 75.9873 ^{o} at the

crossover frequency of 14.7172 rad/s. An analysis for a NN-based adaptive control that augments the LQR controller is presented in Ref. 14.

As compared to the nominal dynamics in (44), the true dynamics considered in this paper are derived as linearized dynamics for a damaged GTM model in which the rudder is off. The unmatched uncertainty for this damaged case is treated in Ref.15 under the assumption that the control input matrix does not change after the damage. In this paper, we assume that the uncertainty in the system matrix A is negligible and that the roll rate model for the damaged GTM is described by:

$$\begin{aligned} \dot{\boldsymbol{x}} &= A\boldsymbol{x} + \alpha(\boldsymbol{b} + \beta\Delta B)\eta(s)u + \boldsymbol{b}_m p_{cmd}, \\ y &= \boldsymbol{c}^\top \boldsymbol{x}, \end{aligned} \tag{44}$$

where β is introduced as another scale factor for simulation study, and $\Delta B = [0.0398, 0.9941, 0.0268]^\top$. Notice that when $\beta > 1.7934$ control reversal occurs for the aileron. The transfer function $\eta(s)$ denotes unmodeled input dynamics which are not considered in the design of the control law in (42), such as servo dynamics, and is given by:

$$\eta(s) = \frac{1}{s/\tau_c + 1}, \tag{45}$$

where $\tau_c = 1$ is the time constant. Compared to (40), the system in (44) can be written as:

$$\dot{\boldsymbol{x}} = A\boldsymbol{x} + \alpha\boldsymbol{b}u + \boldsymbol{b}_m p_{cmd} + B_u\Delta(s)u, \tag{46}$$

where

$$B_u = diag\{0, I_{3\times 3}\}, \Delta(s) = \alpha\left[\boldsymbol{b}(\eta(s) - 1) + \beta\Delta B\eta(s)\right]. \tag{47}$$

The role of the scale factor α can be seen when $\Delta(s)$ is explicitly written as:

$$\Delta(s) = \frac{\alpha}{s + \tau_c}\left[\begin{array}{ccc} 0.0665s + 0.0398\beta\tau_c & 1.7828s + 0.9941\beta\tau_c & 0.0462s + 0.0268\beta\tau_c \end{array}\right]. \tag{48}$$

Since the $\mathcal{L}_2$ gain of $\Delta(s)$ is dominated by the second element in (48), and the magnitude peak for the second element occurs at $\omega = \infty$ unless $\beta\tau_c$ is selected very large in magnitude, without α, the $\mathcal{L}_2$ gain of $\Delta(s)$ remains close to 1.7828 for the modest variations of β. Therefore, employing α allows for the $\mathcal{L}_2$ gain of $\Delta(s)$ be scaled with α as $\|\Delta(s)\|_\infty \approx 1.7828\alpha$. This also lowers the bandwidth of the reference model when the control input becomes less effective as α decreases. Figure 7(a) shows the H_∞ norm variation of $\Delta(s)$ as the scale factor α varies when $\beta = 0.5$. The scale factor β is a measure of input uncertainty whose directions are fixed by ΔB in the input channel. The effect of β on the H_∞ norm of $\Delta(s)$ only shows up when β is large because for small β, the maximal magnitude peak for $\Delta(j\omega)$ occurs at $\omega = \infty$, and therefore the H_∞ norm of $\Delta(s)$ remains flat for modest variation of β. Figure 7(b) illustrates the effect of β variation when $\alpha = 1$. The positive limit for β is set as 1.7934 in Figure 7(b) where aileron reversal occurs.

The dynamics in (46) leads to $\boldsymbol{W} = \boldsymbol{0}_{3\times 1}, \boldsymbol{\phi}(\boldsymbol{x}) = \boldsymbol{x}_p$ where $\boldsymbol{x}_p = [v, p, r]^\top$, when compared to (18). The P matrix in (6) is obtained solving (7) with $Q = 5I_{4\times 4}$. The system matrices considered in (22) for the $\mathcal{L}_2$ gain analysis are:

$$\bar{A}(\boldsymbol{x}) = \left[\begin{array}{cc} A_m & \boldsymbol{b}\boldsymbol{x}_p^\top \\ -\gamma\boldsymbol{x}_p\boldsymbol{b}^\top P & -\sigma I_{3\times 3} \end{array}\right], \bar{B}_p = \left[\begin{array}{c} -B_u \\ 0 \end{array}\right], \bar{C}_p = \left[\begin{array}{cc} \boldsymbol{K}_x^\top + [0, W^\top] & -\boldsymbol{x}_p^\top \end{array}\right]^\top. \tag{49}$$

The compact domain of interest is set as $\Omega_x = [-0.1, 0.1] \times [-0.2, 0.2] \times [-0.05, 0.05]$ for (v, p, r), and $\boldsymbol{W} = \boldsymbol{0}_{3\times 1}$ for LMI analysis. This leads to the following corner set:

$$\mathcal{P}_0^a := \{\boldsymbol{\rho}^a = (v, p, r, \boldsymbol{W}) \ : \ v \in \{-0.1, 0.1\},\ p \in \{-0.2, 0.2\},\ r \in \{-0.05, 0.05\},\ \boldsymbol{W} \in \{\boldsymbol{0}_{3\times 1}\}\}. \tag{50}$$

The tolerable disk size by applying Lemma 1 is shown in Table 3. The theoretical disk size is determined by the ratio between γ/σ. Table 3 reveals that as the ratio γ/σ increases, the tolerable disk size decreases.

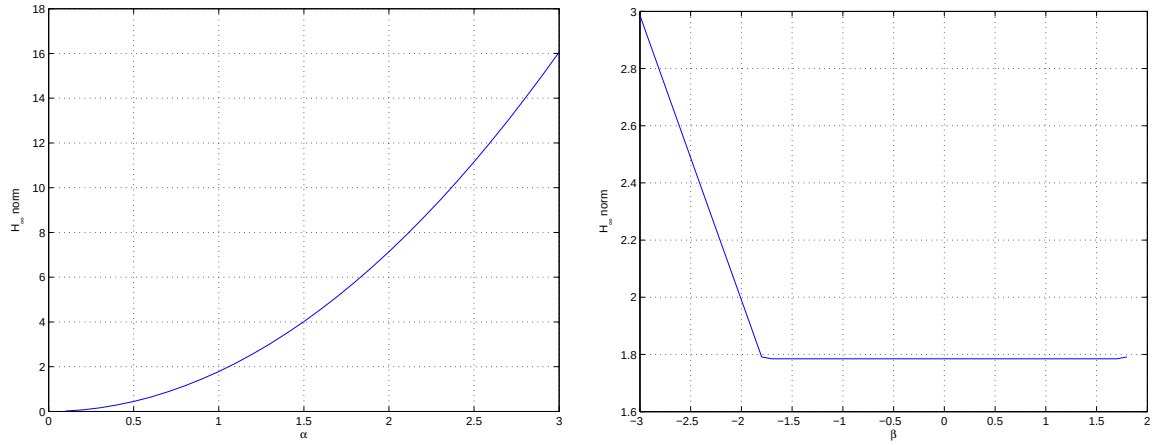

(a) H_∞ norm variation with respect to α with $\beta = 0.5$ fixed

(b) H_∞ norm variation with respect to β with $\alpha = 1$ fixed

Figure 7. H_∞ **norm variation for** $\Delta(s)$

	$\gamma = 0.1$	$\gamma = 1$	$\gamma = 10$	$\gamma = 100$	$\gamma = 1000$
$\sigma = 0.01$	0.2056	0.0559	0.0133	0.0019	0.0004
$\sigma = 0.1$	0.2976	0.2056	0.0559	0.0133	0.0019
$\sigma = 1$	0.3117	0.2976	0.2056	0.0559	0.0133
$\sigma = 10$	0.3131	0.3117	0.2976	0.2056	0.0559
$\sigma = 100$	0.3133	0.3131	0.3117	0.2976	0.2056

Table 3. Tolerable disk size $1/\gamma_s$

For the verification of the results in Table 3, consider the case $\alpha = 0.1$. Figure 8 shows that in this case any combination of (γ, σ) whose tolerable disk size is larger than 0.2056 should remain stable under the variation of $\beta \in [-2, 1.7]$. Figures 9 and 10 show tracking responses when β takes a value either -2.0 or 1.7 when the adaptation gain and the $\sigma-$modification are set as $(1000, 100)$ and $(1, 1)$, respectively. Tracking responses are bounded, which agrees with the corresponding results in Table 3.

At a glance, the conservatism associated with the results in Table 3 may seem investigatable by adjusting α until the adaptive closed-loop system goes unstable while β is fixed. For example, Figure 11 shows tracking responses when $\alpha = 2.0$,while $\beta = 0.5$ is fixed, which leads to $\|\Delta(s)\|_\infty = 3.5693$. However, one underlying assumption in this investigation is that the time constant for the unmodeled dynamics τ_c is fixed as 1. Setting $\tau_c = 0.1$ still makes $\Delta(s)$ retain the same $\mathcal{L}_2$ gain of 3.5693 but leads to drastically different tracking responses shown in Figure 12. This reveals that the H_∞ norm is conservative in that it only considers the worst case and disregards the frequency content in the unmodeled dynamics. This limitation of H_∞ norm makes it difficult to investigate the conservatism associated with the results in Table 3, which remains a future research topic.

V. Conclusions

The framework of LMI-based analysis for adaptive control is applied to a class of systems with unmodeled input dynamics. The formulation involves recasting the error dynamics composed of the tracking error and the weight estimation error into a linear parameter varying form. With the notion of $\mathcal{L}_2$ gain as an metric for robustness of adaptive control to an uncertain dynamic mapping, we show that a broad class of unmodeled

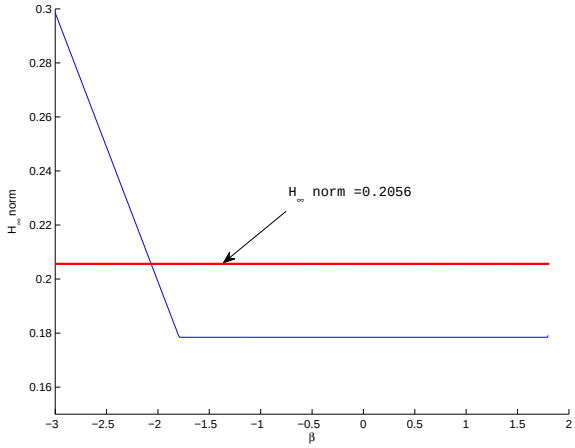

Figure 8. H_∞ **norm variation with respect to** β **with** $\alpha = 0.1$ **fixed**

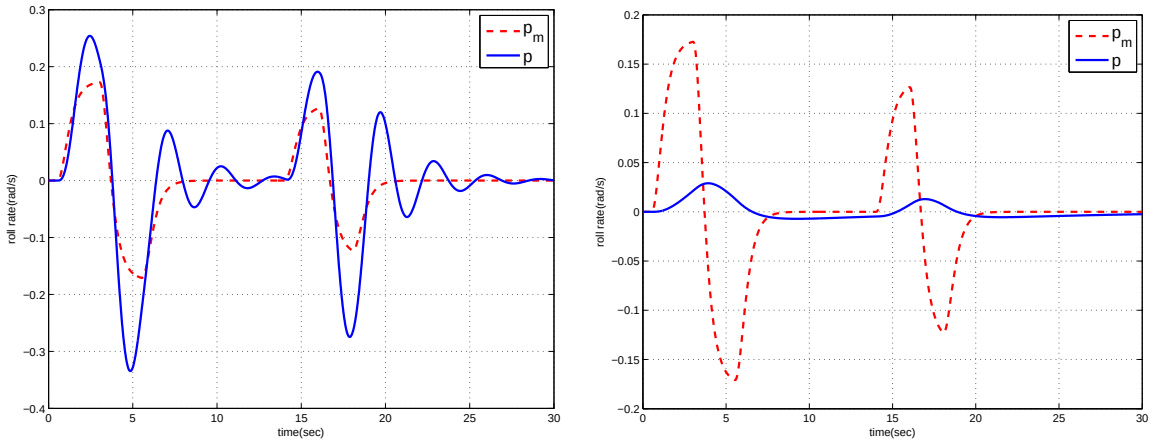

(a) $\beta = -2.0$ (b) $\beta = 1.7$

Figure 9. Tracking responses with $(\gamma, \sigma) = (1000, 100)$

input dynamics can be analyzed under the previously developed LMI framework. The size of tolerable unmodeled input dynamics are quantified by their $\mathcal{L}_2$ gain. It is shown that the LMI framework is a viable tool for analyzing allowable uncertain dynamics that go beyond the class assumed in previous stability margin analysis. The simulation results for the roll rate tracking problem using the Generic Transportation Model illustrates the validity of the $\mathcal{L}_2$ gain analysis and also leads to a requirement for future research on the conservatism associated with this analysis.

VI. Acknowledgments

This research in part was supported under NASA Cooperative Agreement NNX08AC61A.

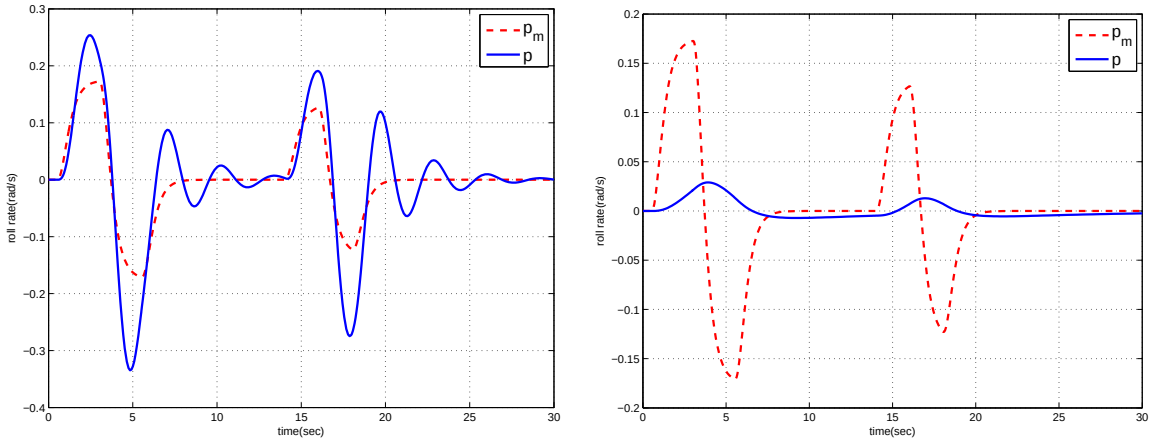

(a) $\beta = -2.0$ (b) $\beta = 1.7$

Figure 10. Tracking responses with $(\gamma, \sigma) = (1, 1)$

References

[1]Narendra, K. and Annaswamy, A., *Stable Adaptive Control*, Prentice-Hall, 1989.

[2]Sastry, S. and Bodson, M., *Adaptive Control: Stability, Convergence, and Robustness*, Prentice-Hall, Englewood Cliffs, NJ, 1989.

[3]Ioannou, P. and Sun, J., *Robust Adaptive Control*, Prentice-Hall, Englewood Cliffs, NJ, 1996.

[4]Marino, R. and Tomei, P., *Nonlinear Control Design: Geometric, Adaptive, & Robust*, Prentice Hall, New Jersey, 1995.

[5]Krstić, M., Kanellakopoulos, I., and Kokotović, P. V., *Nonlinear and Adaptive Control Design*, John Wiley & Sons, New York, 1995.

[6]Tao, G., *Adaptive Control Design and Analysis*, John Wiley & Sons, Hoboken, New Jersey, 2003.

[7]Rohrs, C., Valavani, L., Athans, M., and Stein, G., "Robustness of Continuous-Time Adaptive Control Algorithms in the Presence of Unmodeled Dynamics," *IEEE Transactions on Automatic Control*, Vol. 30, 1985, pp. 881–889.

[8]Ioannou, P. and Kokotović, P., *Adaptive Systems with Reduced Models*, Springer-Verlag, Berlin;New York, 1983.

[9]Naik, S. M., Kumar, P. R., and Ydstie, B. E., "Robust Continuous-Time Adaptive-Control by Parameter Projection," *IEEE Transactions on Automatic Control*, Vol. 37, No. 2, 1992, pp. 182–197.

[10]Lewis, F., Jagannathan, S., and Yeşildirek, A., *Neural Network Control of Robot Manipulators and Nonlinear Systems*, Taylor & Francis, 1999.

[11]Spooner, J. T., Maggiore, M., Ordóñez, R., and Passino, K. M., *Stable Adaptive Control and Estimation for Nonlinear Systems- Neural and Fuzzy Approximator Techniques*, John Wiley & Sons, New York, NY, 2002.

[12]Calise, A. J., Lee, S., and Sharma, M., "Development of a reconfigurable flight control law for tailless aircraft," *Journal of Guidance, Control, and Dynamics*, Vol. 24, No. 5, 2001, pp. 896–902.

[13]Yang, B.-J., Yucelen, T., Calise, A. J., and Shin, J.-Y., "LMI-based analysis of adaptive controllers," *Proceedings of the American Control Conference*, St. Louis, MO, 2009.

[14]Yang, B. J., Yucelen, T., Calise, A., and Shin, J., "An LMI-based Analysis of Stability Margins in Adaptive Flight Control," *AIAA Guidance, Navgation, and Control Conference*, Chicago, IL, 2009.

[15]Yang, B. J., Yucelen, T., Shin, J., and Calise, A. J., "An LMI-based Analysis of an Adaptive Flight Control System with Unmatched Uncertainty," *AIAA Infotech@Aerospace*, AIAA 2010-3436, Atlanta, GA, April 2010.

[16]Khalil, H., *Nonlinear Systems*, Prentice-Hall, Upper Saddle River, NJ, 1996.

[17]Franklin, G., Powell, J., and Emami-Naeini, A., *Feedback Control of Dynamic Systems*, Addison-Wesley, 1995.

[18]Zhou, K. and Doyle, J. C., *Essentials of robust control*, Prentice Hall, Upper Saddle River, N.J., 1998.

[19]Sepulchre, R., Janković, M., and Kokotović, P., *Constructive nonlinear control*, Springer, New York, 1997.

[20]Desoer, C. A. and Vidyasagar, M., *Feedback systems: input-output properties*, Academic Press, New York,, 1975.

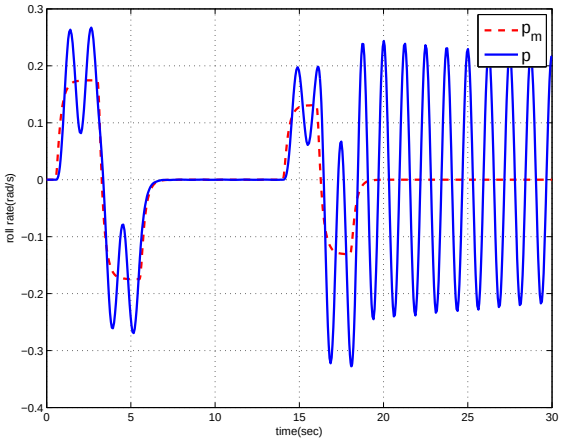

(a) $\gamma = 0.1$

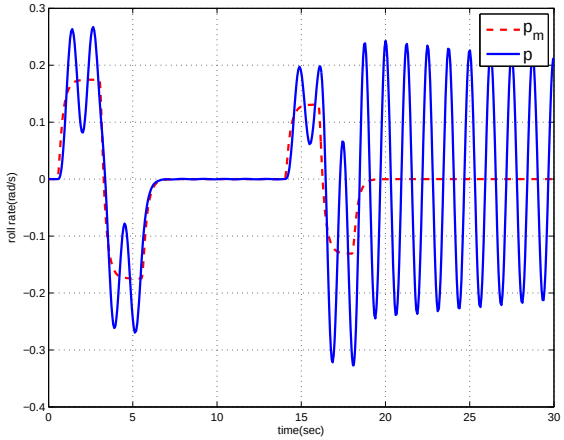

(b) $\gamma = 1.0$

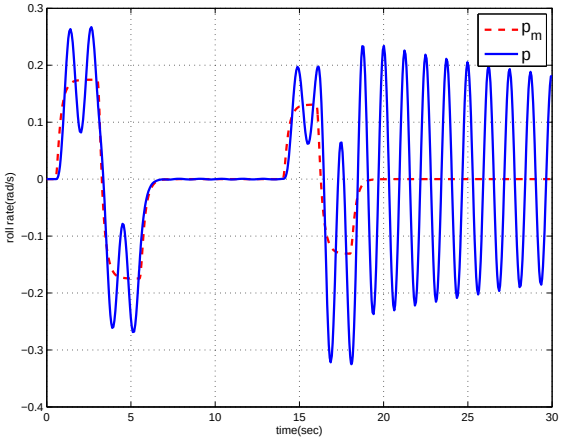

(c) $\gamma = 10.0$

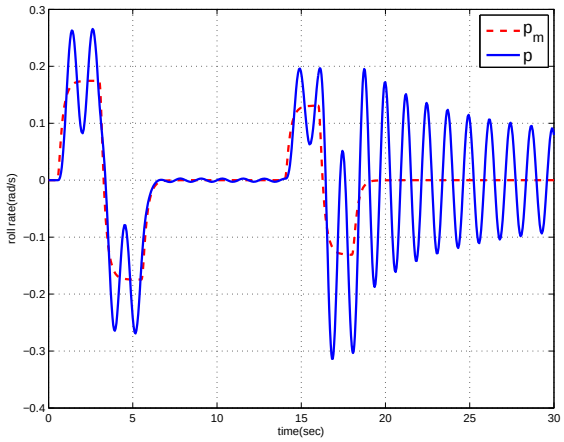

(d) $\gamma = 100.0$

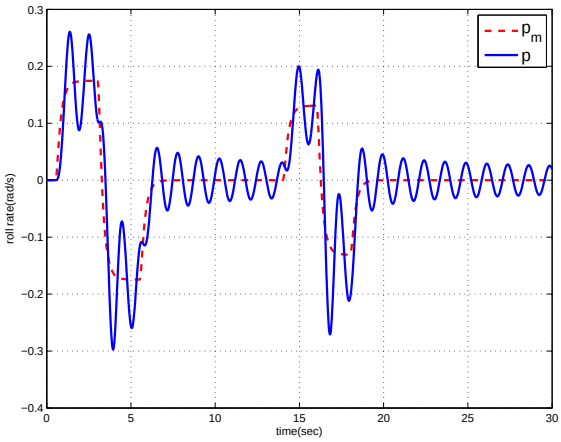

(e) $\gamma = 1000.0$

Figure 11. Tracking responses with $\alpha = 2.0$ and $\tau_c = 1$

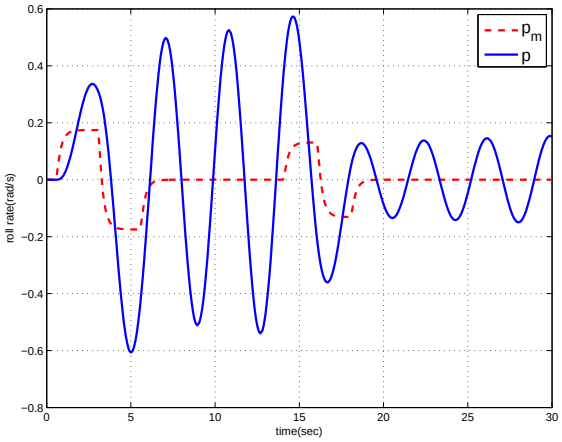

(a) $\gamma = 0.1$

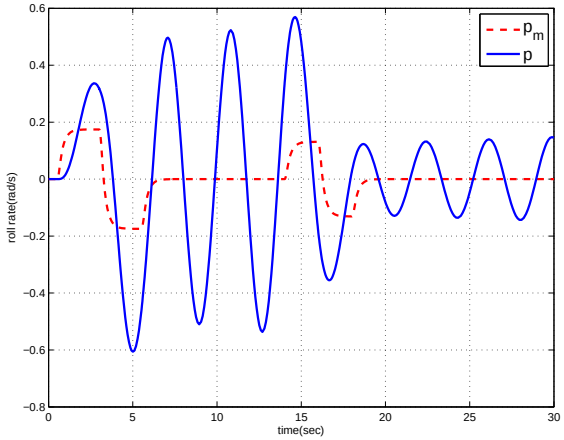

(b) $\gamma = 1.0$

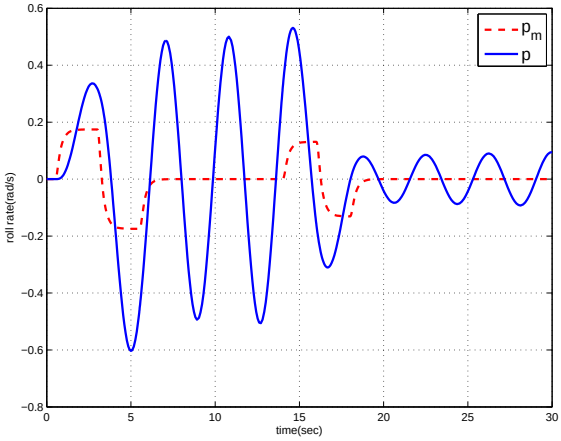

(c) $\gamma = 10.0$

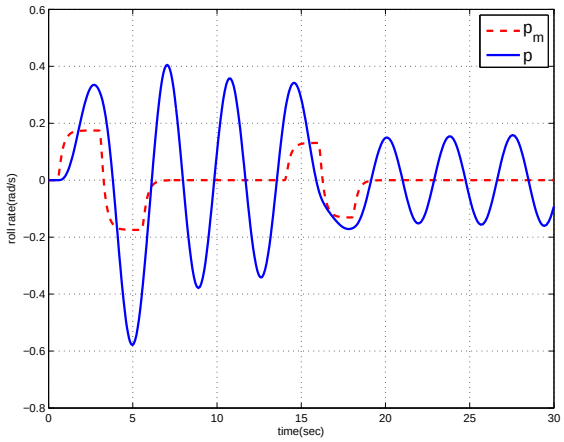

(d) $\gamma = 100.0$

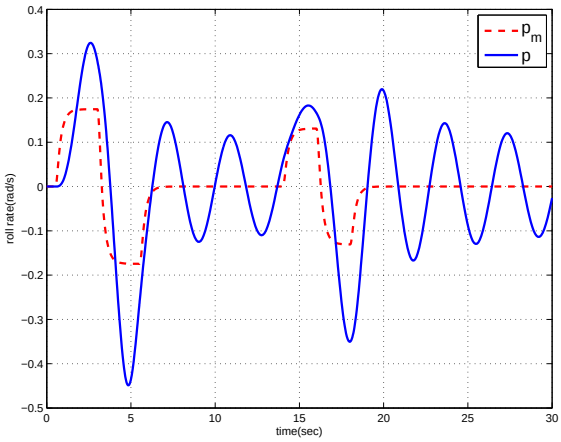

(e) $\gamma = 1000.0$

Figure 12. Tracking responses with $\alpha = 2.0$ and $\tau_c = 0.1$